AIP | Applied Physics Letters

Strong coupling between Rhodamine 6G and localized surface plasmon resonance of immobile Ag nanoclusters fabricated by direct current sputtering

Yingcui Fang, Kevin Blinn, Xiaxi Li, Guojun Weng, and Meilin Liu

Citation: Appl. Phys. Lett. **102**, 143112 (2013); doi: 10.1063/1.4801633
View online: http://dx.doi.org/10.1063/1.4801633
View Table of Contents: http://apl.aip.org/resource/1/APPLAB/v102/i14
Published by the American Institute of Physics.

Strong coupling between Rhodamine 6G and localized surface plasmon resonance of immobile Ag nanoclusters fabricated by direct current sputtering

Yingcui Fang,[1,2,a)] Kevin Blinn,[1] Xiaxi Li,[1] Guojun Weng,[3] and Meilin Liu[1,b)]
[1]*School of Materials Science and Engineering, Center for Innovative Fuel Cell and Battery Technologies, Georgia Institute of Technology, Atlanta, Georgia 30332-0245, USA*
[2]*Vacuum Section, Hefei University of Technology, Hefei, Anhui 230009, China*
[3]*The Key Laboratory of Biomedical Information Engineering of Ministry of Education, School of Life Science and Technology, Xi'an Jiaotong University, Xi'an 710049, China*

(Received 11 February 2013; accepted 27 March 2013; published online 10 April 2013)

We made clean silver nano-clusters (AgNCs) on glass substrates by DC magnetron sputtering of a high purity Ag target in a high vacuum chamber. The AgNCs film shows strong localized surface plasmon resonance (LSPR) due to the coupling among Ag nanoparticles in the AgNCs and the coupling between AgNCs. The LSPR indicates strong coupling with Rhodamine 6G (R6G) adsorbed on the AgNC surface, which enhances the R6G absorption intensity and broadens the absorption wavelength range. This result promotes plasmonic nanoparticles to be better used in solar cells. © *2013 AIP Publishing LLC*. [http://dx.doi.org/10.1063/1.4801633]

Ag nanoparticles (AgNPs) produce a sharp and strong localized surface plasmon resonance (LSPR),[1] if given a proper visible light excitation. Recently, plasmonic enhancement of the efficiencies of solar cells[2–5] and organic light emitting diodes[6,7] is drawing tremendous interest. Promoting light absorption[8,9] is one of the key issues improving the solar cell efficiency. Historically, most plasmonic nanoparticles have been synthesized with colloidal chemical methods[10] or monolayer assembly by Langmuir-Blodgett technique.[11] Other methods are based on lithographic techniques such as electron beam[12] or nanosphere lithography.[13] Previous work has also demonstrated that when two or more AgNPs are brought into proximity, the LSPR of individual AgNPs couples each other, resulting in enhanced LSPR intensity and modulated peak position,[14] which would benefit us to better use of LSPR. But again, most reported coupled plasmonic particles were produced by chemical seeding techniques[15] or electron beam lithography.[16] Magnetron sputtering[17] is a very common technology to produce nanoparticles free from chemical residues. The clean nanoparticles allow the probe molecules to be directly adsorbed on the nanoparticle surface, which is favorable for strong coupling between the LSPR and the excitons of the adsorbed molecules to take place. Strong coupling benefits energy transfer and charge transfer and hence could enhance the energy transfer efficiency in solar cells.

Our group has previously produced AgNPs on silicon substrates by DC sputtering and studied their surface enhanced Raman scattering (SERS) enhancement properties using Rhodamine 6G (R6G).[18] Most AgNPs on silicon substrates isolated from each other to form three dimensional nanostructures. These unique structures had high SERS activity and were successfully applied to detect carbon deposition and cathode thin film materials used in solid oxide fuel cells.[19] For the current work, AgNPs were deposited on glass substrates by DC sputtering. The morphology of the AgNPs has been successfully changed from "isolated row" to "nanocluster" and then to thin continuous smooth films with sputtering time increase from 40 s to 300 s at sputtering power of 10 W. The nanoclusters showed the strongest LSPR and the strongest coupling with the excitons of R6G. This study provides useful information for improving efficiency of solar cell and organic light emission diodes.

The AgNPs films were deposited onto glass substrates by a 10 W DC sputtering level using a high purity Ag target (99.995%) with a plasma generated by ultra-purity Ar (99.999%) at sputtering times of 40, 100, 180, and 300 s. The base pressure in the vacuum chamber was about 2×10^{-6} mbar. During sputtering, the flow of Ar was 80 sccm, and the working pressure was maintained at 2.2×10^{-2} mbar. The substrates themselves were not heated during sputtering. After deposition the samples were removed from the vacuum chamber and immersed in R6G solution with a concentration of 10^{-5} M for 3 h. The morphology and uniformity of the films were characterized by atomic force microscopy (AFM). Extinction spectra were measured by an Ocean Optics HR4000Cg-UV-NIR spectrometer.

AFM images of AgNPs deposited on glass substrates by sputtering at 10 W for 40, 100, 180, and 300 s (named 10W40s, 10W100s, 10W180s, and 10W300s in the following) are shown in Figs. 1(a)–1(d), respectively. The AgNPs of the 10W40s sample are ellipsoids with size dispersion. Some small ones are about 10 nm, and the largest can reach 40 nm. The long axis of most particles is roughly along the same direction such that "nano-row"-like structures are formed, with spaces between rows. The characteristic features of the AgNPs deposited at sputtering time of 100 s are "nanoclusters," composed of two or three small silver nanospheres with an average size around 16 nm each. The preferential direction is still obvious. When the sputtering time was increased to longer than 180 s, there were no obvious

a)ycfang@ustc.edu.cn. Tel.: +86-551-62901326. Fax: +86-551-62903450.
b)Meilin.liu@gatech.edu.cn

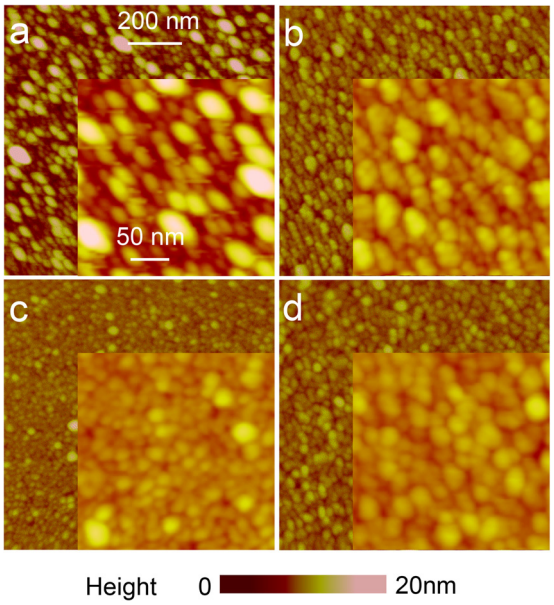

FIG. 1. AFM images of AgNPs samples fabricated at DC sputtering power of 10 W for sputtering times of (a) 40 s, (b) 100 s, (c) 180 s, and (d) 300 s. The scale bars are same for the four figures.

clusters on the surface. The AgNPs were spherical with average size around 20 and 30 nm for sputtering for 180 and 300 s, respectively. The AgNPs connected tightly to form continuous thin films with smooth surface, which is much different from AgNPs on silicon surface.[18]

The growth of AgNPs by sputtering has been widely studied.[20] It follows a Volmer-Weber growth mode:[21] in the initial state, the Ag atoms reaching the substrate form isolated nuclei on the surface. After the nuclei formation process, the subsequently reached atoms diffuse on the surface and join the formed nuclei to promote their growth. This is nuclei growth. As the sputtering time increases, the nanoclusters coalesce into a continuous film.[22] We found the right fabrication parameters and clearly recorded this process. In our experiment, we chose 10 W as the sputtering power level, and when sputtering for 40 s, we observed the isolated nuclei. Most particles are ~10 nm, and a few larger ones have a size of about 40 nm, which are in fact grown nuclei. Even though some parts of the glass surface are still blank with gaps between the 10 nm-AgNPs, the subsequently arrived Ag atoms do not form nuclei in the gaps; instead, they diffuse across the surface to join the formed nuclei and promote the nuclei to grow into clusters. When sputtering for 100 s, a clear image of the grown clusters was obtained, as shown in Fig. 1(b). The formed clusters are composed of two or three nanospheres, while the gaps between adjacent clusters are very small. Such structure is very favorable for producing strong LSPR due to the coupling among the AgNPs in the clusters and the coupling between the AgNCs. It indeed owns strong LSPR and will be demonstrated later. The deposited clusters changed the surface energy such that the subsequently reached atoms would be easily trapped at the gaps and form nuclei. Therefore, when the sputtering time was increased to 180 s, the surface became smooth and no clusters could be seen, which is shown in Fig. 1(c). As sputtering time was

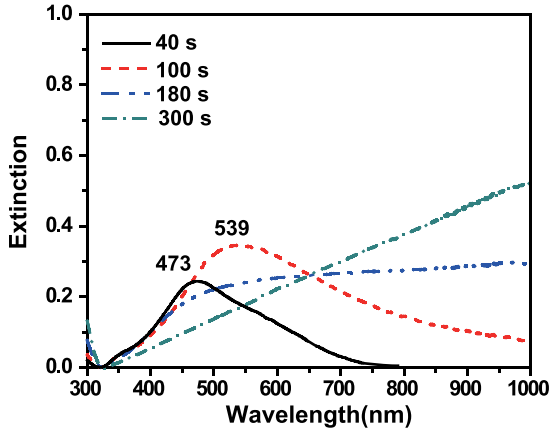

FIG. 2. The extinction spectra of AgNPs deposited on glass substrates by sputtering at 10 W for times of 40, 100, 180, and 300 s.

increased further to 300 s, the particles grow further to ~30 nm due to the Ostwald ripening process.[23]

The extinction spectra of AgNP films with different sputtering times are shown in Fig. 2. The 10W40s sample had an asymmetric LSPR peak at 473 nm, and the LSPR peak shifted to 539 nm with a stronger intensity as the sputtering time was increased to 100 s. When the sputtering time was further increased to 180 s, a broad band that covered the whole range of the measurement was obtained. This band had a shoulder around 539 nm. Compared with that of the 10W100s sample, the extinction spectrum of the 10W180s sample showed higher absorption at longer wavelength range (670–1000 nm) but lower intensity at shorter wavelength range (300–670 nm). When the sputtering time was increased to 300 s, the absorption spectrum turned into a straight line.

The extinction spectra of the samples are related to the morphology of the sputtered AgNPs. The average particle size of the 10W100s sample is 16 nm, and the corresponding LSPR peak is located at 539 nm. Comparatively, Futamata[24] reported that isolated 16 nm AgNPs gave an absorption peak at 397 nm which shifted to longer wavelength when the AgNPs were brought closer to each other. For example, in the case of three AgNPs with 1-nm gaps between them, the LSPR shifted to 600 nm, while with a 2 nm-gap, the LSPR peak was found at 510 nm. Based on the above report and the AFM images shown in Figs. 1(a) and 1(b), the observed LSPR peaks at 473 nm and 539 nm in this study were due to the coupling among AgNPs in a cluster and the coupling between AgNCs. Especially for the 10W100s sample, the gaps between clusters are very narrow. These narrow gaps are very important and are hotspots which own huge electric field due to the coupling between the isolated AgNCs.

As shown in Fig. 1(c), the AgNPs in the 10W180s sample had an average particle size of 20 nm. Since the nanoparticles connected one by one to form smooth continual film the LSPR in fact turned into surface plasmon (SP), therefore the extinction intensity was reduced and there was no absorption peak in the absorption spectrum but a shoulder at 539 nm. Sputtering for 300 s, the particle size increased to 30 nm; however, due to the connection of AgNPs, the film turned into 2-dimensional continual films. Reflection from the films seriously interfered with the measurement.

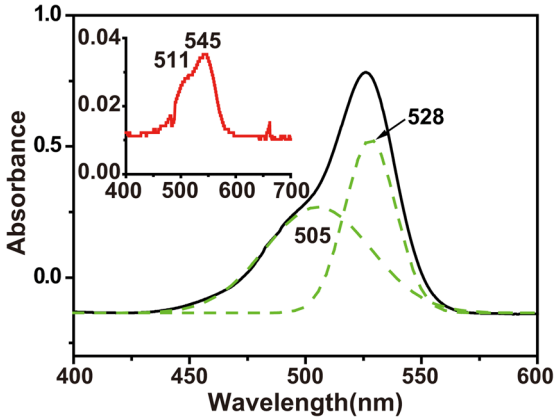

FIG. 3. The absorption spectra of 10^{-5}M concentration R6G in water, and on the surface of glass substrates (inset).

Before we discuss the coupling between the LSPR and the excitons of R6G, the absorption spectrum of R6G was explored. Fig. 3 provides the absorption spectra of 10^{-5}M R6G in water and the deconvolution of the spectrum with two Gaussian curves centered at 505 and 528 nm (dashed line). The 528 nm peak was assigned to the S_0-S_1 electronic transition, while the 505 nm was due to the vibronic S_0-S_1 transition[25] and might be overlapped by absorption of H-dimers.[26] When R6G molecules were adsorbed on the surfaces of glass substrates and dried in air, the extinction spectra changed very much, as shown in the inset in Fig. 3. The intensity was dramatically reduced and the two peaks shifted from 505 to 511 nm and from 528 to 545 nm. The redshift of the R6G resonant peak was caused by the change of the dielectric environment from water to glass.[27]

When R6G molecules were loaded onto the surface of AgNPs, the extinction spectra changed much. Fig. 4(a) shows the extinction spectra of AgNP films sputtering for 40, 100, 180, and 300 s after the samples were vertically dipped in 10^{-5}M R6G solution for 3 h and dried in air. The 10W40s, 10W100s, and 10W180s samples showed a three-peak feature and the 10W300s sample showed only two peaks. The highest-energy peak showed a redshift from 446 to 459 nm and then blueshifted to 444 nm, while the lowest-energy peak red shifted from 574 to 593 nm and then blue-shifted to 557 and to 553 nm as the sputtering time was increased from 40 to 300 s. For the three-peak samples, as the peak redshifted, the absorption intensity increased and the distance between the highest-energy and lowest-energy peaks increased from 128 to 134 nm. With the blueshift of the peak, the absorption intensity was decreased, accompanied by a distance decrease from 134 to 113 nm.

It is clear that when R6G molecules were absorbed on the AgNPs surface, the resultant absorption spectra were not the simple overlap of the R6G spectrum and the LSRP of AgNPs. Chen *et al.*[28] gave a detailed review about the interaction between LSPR and organic molecules. If molecules exhibit strong absorption around the LSPR of metal nanocrystals, plasmonic-molecular resonant coupling will take place and the hybridization of the plasmonic and molecular resonances result in distinct spectral properties in comparison with those of the separate constituents. Cade[29] reported

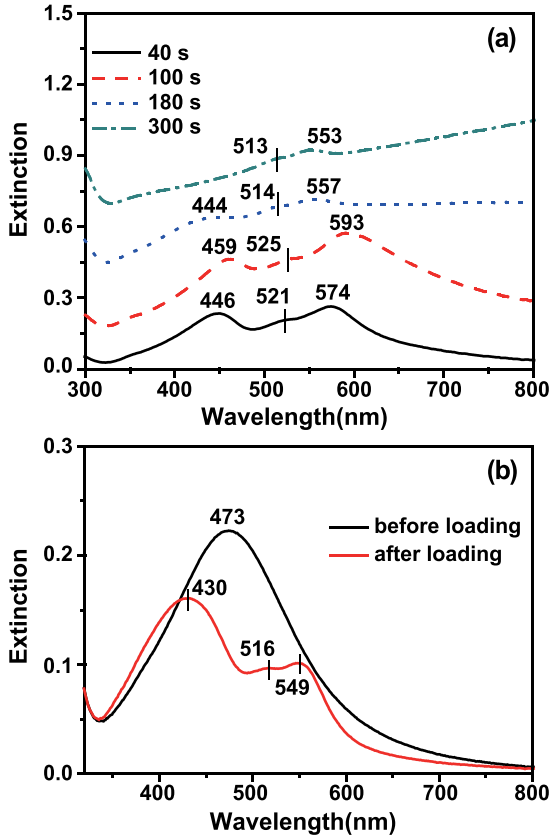

FIG. 4. The extinction spectra of AgNP films made by sputtering for 40, 100, 180, and 300 s after the samples were vertically dipped in 10^{-5}M R6G solution for 3 h and dried in air (a), and the extinction spectra of AgNP films made by vacuum evaporation before and after loaded with 10^{-5}M R6G (b).

strong coupling between the excitons of R6G and the LSPR of AgNPs fabricated by vacuum evaporation. The hybridization of the excitons of R6G and the plasmon of AgNPs gave rise to three polariton peaks. The three polariton peaks redshifted as film thickness increase and the resulting polariton dispersion curves manifested as an anti-crossing behavior.

In this work, the LSPR of the 10W40s, 10W100s, and 10W180s samples showed strong coupling with the excitons of 10^{-5}M R6G because all three peaks in the adsorption spectra could be attributed to polaritons. As sputtering time increased, the coupling got stronger: the intensities increased and the peaks redshifted. However, when the sputtering time was 180 s or longer, the coupling effect decreased: the intensities decreased and the peaks blueshifted. Therefore, the AgNPs coupled strongly with the excitons of R6G when sputtering time was no longer than 180 s, and the strongest coupling effect took place between AgNCs and the R6G. We will further discuss it in the following.

The absorption band of 10^{-5}M R6G is in the wavelength range from 450 to 550 nm with maximal absorption around 538 nm. According to Fig. 2, the LSPR of the 10W40s, 10W100s, and 10W180s samples are within this range. Thus, the excitons of R6G and the LSPR of these AgNPs can be coupled resonantly.[30] Since the LSPR of the 10W100s AgNCs is the strongest and its location is near the maximal absorption of R6G, the coupling is the strongest.

The weaker coupling between R6G and the AgNP films when the sputtering time was over 100 s could be attributed

to three factors. First, due to the continuity of the formed AgNP thin film the LSPR was in fact turn into SP, which was much weaker than the LSPR. Second, due to the coupling among AgNPs the SP was in the infrared region; therefore, the excitons of the R6G molecules could not resonantly couple with the plasmons. Chen *et al.*[28] reported that when the wavelength of LSPR was much longer than that of the molecular absorption, the coupling became very weak. In this situation, the role of the molecules was only changing the dielectric constant of the nano environment surrounding metal nanocrystals. The absorption peak of R6G was just overlapped on the right side of the LSPR of the 10W300s AgNPs thin film; therefore, no strong coupling took place. Third, the reduced surface area in the AgNP samples with longer sputtering time might promote the adsorption of R6G in the form of dimers, which would decrease the probability of coupling. For a specific R6G concentration, the amount of dimers would theoretically increase if the specific surface area of total AgNPs was reduced. According to Fig. 1, the 10W100s AgNCs have the largest surface area, and with the sputtering time increase, the roughness was reduced and the total specific surface area was reduced; therefore, the amount of dimers should have increased. When 10^{-5}M R6G molecules were loaded onto Ag film, it was previously reported[26] that the absorption peak of H-dimer was at 506 nm, while the peaks of monomers and J-dimers were at 537 and 568 nm, respectively. In our experiment, the H-dimer absorption peak is near 506 nm, which is consistent with what was reported in the literature. In contrast, the monomer absorption peak is at 553 nm, which is likely due to the mixed absorption of the J-dimers and the monomers. J-aggregates were previously reported to be strongly[31] or coherently[32] coupled with the LSPR of AgNPs, but there are no reports about the strong coupling between H-dimers with LSPR. Therefore, the coupling between SP and the excitation of dimers should be weaker than that of LSPR with the excitons of R6G monomers; hence, the coupling decreased gradually when the sputtering time was longer than 180 s.

For comparison, we also made AgNPs thin film by evaporation in vacuum and tuned the LSPR of the AgNPs to 473 nm, which is at the same wavelength of the 10W40s sample. After loading of 10^{-5}M R6G, the extinction spectrum is shown in Fig. 4(b). The three coupled peaks are located at 430, 516, and 549 nm. It is clear that the coupling between AgNPs made by vacuum evaporation is much weaker than the counterpart made by vacuum sputtering. Therefore, the AgNCs made by vacuum sputtering indeed own very strong LSPR and not only improve the absorption intensity but also broaden the absorption wavelength range of R6G. This technology can be optimized to promote plasmonic nanoparticles to be better used in solar cells.

This work was supported partly by the HeteroFoaM Center, an Energy Frontier Research Center funded by the U.S. Department of Energy, Office of Science, Office of Basic Energy Sciences under Award No. DE-SC0001061 and partly by the National Natural Science Foundation of China (No. 11147027).

[1]P. K. Jain, X. H. Huang, I. H. El-Sayed, and M. A. El-Sayed, Acc. Chem. Res. **41**, 1578 (2008).
[2]A. V. Zayats, I. I. Smolyaninov, and A. A. Maradudin, Phys. Rep. **408**, 131 (2005).
[3]Q. Q. Gan, F. J. Bartoli, and Z. H. Kafafi, IEEE Photonics J. **4**, 620 (2012).
[4]P. Spinelli, V. E. Ferry, J. van de Groep, M. van Lare, M. A. Verschuuren, R. E. I. Schropp, H. A. Atwater, and A. Polman, J. Opt. **14**, 024002 (2012).
[5]M. D. Brown, T. Suteewong, R. S. S. Kumar, V. D'Innocenzo, A. Petrozza, M. M. Lee, U. Wiesner, and H. J. Snaith, Nano Lett. **11**, 438 (2011).
[6]W. H. Koo, S. M. Jeong, S. Nishimura, F. Araoka, K. Ishikawa, T. Toyooka, and H. Takezoe, Adv. Mater. **23**, 1003 (2011).
[7]F. Liu and J. M. Nunzi, Org. Electron. **13**, 1623 (2012).
[8]W. B. Hou, P. Pavaskar, Z. W. Liu, J. Theiss, M. Aykol, and S. B. Cronin, Energy Environ. Sci. **4**, 4650 (2011).
[9]C. Hägglund and S. P. Apell, J. Phys. Chem. Lett. **3**, 1275 (2012).
[10]S. Nie and S. R. Emory, Science **275**, 1102 (1997).
[11]A. Tao, F. Kim, C. Hess, J. Goldberger, R. R. He, Y. G. Sun, Y. N. Xia, and P. D. Yang, Nano Lett. **3**, 1229 (2003).
[12]C. Tabor, R. Murali, M. Mahmoud, and M. A. El-Sayed, J. Phys. Chem. A **113**, 1946 (2009).
[13]A. J. Haes, J. Zhao, S. L. Zou, C. S. Own, L. D. Marks, G. C. Schatz, and R. P. Van Duyne, J. Phys. Chem. B **109**, 11158 (2005).
[14]W. Rechberger, A. Hohenau, A. Leitner, J. R. Krenn, B. Lamprecht, and F. R. Aussenegg, Opt. Commun. **220**, 137 (2003).
[15]P. K. Jain, S. Eustis, and M. A. El-Sayed, J. Phys. Chem. B **110**, 18243 (2006).
[16]K. H. Su, Q. H. Wei, X. Zhang, J. J. Mock, D. R. Smith, and S. Schultz, Nano Lett. **3**, 1087 (2003).
[17]W. Crookes, Proc. R. Soc. London **50**, 88 (1891).
[18]Y. C. Fang, X. X. Li, K. Blinn, M. A. Mahmoud, and M. L. Liu, J. Vac. Sci. Technol. A **30**, 050606 (2012).
[19]X. X. Li, K. Blinn, Y. C. Fang, M. F. Liu, M. A. Mahmoud, S. Cheng, L. A. Bottomley, M. EI-Sayed, and M. L. Liu, Phys. Chem. Chem. Phys. **14**, 5919 (2012).
[20]S. Kunduy, S. Hazray, S. Banerjeey, M. K. Sanyaly, S. K. Mandalz, S. Chaudhuriz, and A. K. Palz, J. Phys. D: Appl. Phys. **31**, L73 (1998).
[21]L. Eckertova, *Physics of Thin Films* (Plenum Press, New York, 1986).
[22]C. Charton and M. Fahland, Vacuum **68**, 65 (2002).
[23]J. W. Bullard, Mater. Sci. Eng., A **238**, 128 (1997).
[24]M. Futamata and Y. Maruyama, Appl. Phys. B **93**, 117 (2008).
[25]P. Hildebrandt and M. Stockburger, J. Phys. Chem. **88**, 5935 (1984).
[26]J. Zhao, L. Jensen, J. H. Sung, S. L. Zou, G. C. Schatz, and R. P. Van Duyne, J. Am. Chem. Soc. **129**, 7647 (2007).
[27]E. Ringe, J. M. McMahon, K. Sohn, C. Cobley, Y. N. Xia, J. X. Huang, G. C. Schatz, L. D. Marks, and R. P. Van Duyne, J. Phys. Chem. C **114**, 12511 (2010).
[28]H. J. Chen, T. A. Ming, L. Zhao, F. Wang, L. D. Sun, J. F. Wang, and C. H. Yan, Nanotoday **5**, 494 (2010).
[29]N. I. Cade, T. Ritman-Meer, and D. Richards, Phys. Rev. B **79**, 241404R (2009).
[30]P. Spinelli and A. Polman, Opt. Express **20**, A641 (2012).
[31]C. Bonnand, J. Bellessa, and J. C. Plenet, J. Non-Cryst. Solids **352**, 1683 (2006).
[32]G. P. Wiederrecht, G. A. Wurtz, and J. Hranisavljevic, Nano Lett. **4**, 2121 (2004).